



Two phase flow redistribution in a two-layered porous medium with contrasting permeability

Ali Swaidan, Florian Fichot, Michel Quintard

► To cite this version:

Ali Swaidan, Florian Fichot, Michel Quintard. Two phase flow redistribution in a two-layered porous medium with contrasting permeability. 7th International Symposium on Advances in Computational Heat Transfer, May 2017, Napoli, Italy. pp.441-462. hal-03624241

HAL Id: hal-03624241

<https://hal.science/hal-03624241>

Submitted on 30 Mar 2022

HAL is a multi-disciplinary open access archive for the deposit and dissemination of scientific research documents, whether they are published or not. The documents may come from teaching and research institutions in France or abroad, or from public or private research centers.

L'archive ouverte pluridisciplinaire **HAL**, est destinée au dépôt et à la diffusion de documents scientifiques de niveau recherche, publiés ou non, émanant des établissements d'enseignement et de recherche français ou étrangers, des laboratoires publics ou privés.




Open Archive TOULOUSE Archive Ouverte (OATAO)

OATAO is an open access repository that collects the work of Toulouse researchers and makes it freely available over the web where possible.

This is an author-deposited version published in : <http://oatao.univ-toulouse.fr/>
Eprints ID : 19966

To link to this article : DOI:10.1615/ICHMT.2017.460
URL : <http://dx.doi.org/10.1615/ICHMT.2017.460>

To cite this version : Swaidan, Ali and Fichot, Florian and Quintard, Michel  *Two phase flow redistribution in a two-layered porous medium with contrasting permeability*. (2017) In: 7th International Symposium on Advances in Computational Heat Transfer, 28 May 2017 - 2 June 2017 (Napoli, Italy).

Any correspondence concerning this service should be sent to the repository administrator: staff-oatao@listes-diff.inp-toulouse.fr

Two phase flow redistribution in a two-layered porous medium with contrasting permeability

Ali Swaidan^{§,a}, Florian Fichot^a, M. Quintard^b

^aInstitut de Radioprotection et de Sûreté Nucléaire (IRSN) - PSN-RES/SAG/LEPC - Cadarache bât. 702 - 13115 St Paul-lez-Durance, FRANCE

^bUniversité de Toulouse - INPT - UPS - Institut de Mécanique des Fluides de Toulouse (IMFT) - Allée Camille Soula, F-31400 Toulouse, FRANCE

§ Corresponding author. Email: ali.swaidan@irsn.fr

ABSTRACT Motivated to investigate debris bed coolability in a damaged nuclear reactor core by bottom reflooding, this paper studies the physical situation involving injection of water into a superheated particle bed leading to high velocity flow of steam. The particle bed is composed of two cylindrical concentric parts and stratified vertically. One of the particular features of the studied configuration is that quenching of the superheated particles generates a strong flow of steam which may create a vertical pressure gradient leading the water in the lateral, more permeable medium, to flow faster than the injection velocity and consequently reducing the efficiency of cooling. The aim is to propose an analytical model to predict the behavior of water entrainment in the lateral layer (bypass) of larger permeability and porosity. This model computes the quench front velocity, water-to-steam conversion ratio, and the velocity of water in the bypass. It provides good qualitative and quantitative results for the two-phase flow redistribution as compared to experimental data. It also has several advantages as it allows: performing fast evaluations of the efficiency of cooling, upscaling to reactor-scale straightforwardly, and performing sensitivity studies on the physical properties of the particle beds and the fluid, and the variations of the momentum equations. For instance, it showed that the Generalized Darcy law was not sufficient to obtain acceptable evaluations whereas considering non-zero cross-terms in the Darcy Forchheimer equation by including an interfacial friction law succeeds in obtaining better results.

Keywords: Reflooding, Two-phase flow, Porous media, Bypass, Water entrainment

Nomenclature

symbol	variables	units
α	void fraction	
ε	porosity	
ϕ	mass flow rate	kg/s
κ	absolute permeability	m^2
η	absolute passability	m
v	absolute velocity	m/s
U	superficial velocity	m/s
z	elevation in the porous medium	m
d_p	particles diameter	m
S^i	cross section area	m^2
$\Delta T_f = T_f - T_{sat}$	temperature difference	K
subscripts		
g	gas	
l	liquid	
s	solid	
superscripts		
c	bypass	
b	center	
inj	injection	
qf	quench front	

Introduction

Debris Bed Formation Following a loss of coolant accident in a PWR (pressurized water reactor), the reactor core gets uncovered and starts to accumulate residual heat. As the accident evolves, core heating and oxidation of the fuel cladding by the coolant vapor provoke core degradation. In this case reflooding the core can cause a thermal shock and the embrittlement of the cladding, hence forming a porous debris bed in the core. Severe accidents arising from the fusion of the nuclear reactor core must be anticipated to enhance the efficiency of its mitigation. Such accidents have occurred in Chernobyl-1984, at the Three Mile Island unit-2 (TMI-2) in the USA-1979, and recently in Fukushima, Japan-2011 where 3 reactors were destroyed. The concept of debris bed formation was introduced by Akers and McCardell (1989) and McCardell et al. (1990) upon the post-accident examination of the Three Mile Island unit-2 (TMI-2) that occurred in the USA-1979. In the latter accident, the debris bed composed particle of sizes ranging over few millimeters (Akers et al. (1986), Broughton et al. (1989)) due to the relocation of molten materials inside the core upon quenching of the very hot rods being uncovered. In such situations different debris bed configurations might exist such as the formation of a debris bed surrounded by an intact zone of fuel rods or the existence of compact zones of very small particles limiting the coolant penetration.

Debris Bed Coolability The reflooding models used for Loss of Coolant Accident (LOCA) are not applicable for debris bed cooling. And as severe accident management is crucial, the question of debris coolability has to be resolved. Several experimental programs on debris coolability have been performed over the last decades following the TMI accident, aiming at determining the maximum power that can be extracted from a heated debris bed by water reflooding. Top and bottom

reflooding experiments were performed (Hofmann (1984), Tutu et al. (1984), Reed et al. (1985), and Hu and Theofanous (1991)). And more recently debris bed coolability is again under investigation with experimental programs such as DEBRIS (Schäfer et al. (2006)) at IKE in Germany, PRELUDE and PEARL (Stenne et al. (2009), Repetto et al. (2011), Repetto et al. (2013), and Chikhi et al. (2015)) which were launched by IRSN to investigate the thermal hydraulics of the reflooding process and develop new reflooding models and to validate 2D/3D models. The aim is to predict the consequences of the water reflooding of a severely damaged reactor core where a large part of the core has collapsed and formed a debris bed.

The Scope and System Under Study Modeling two-phase flow in stratified heterogeneous porous media is a problem often investigated in several scientific fields such as petroleum engineering, hydrology, and soil science. Different mathematical models to describe the Darcian and inertia flow of two immiscible phases in a porous medium were proposed in the literature. While upscaling methods applied to the pore-scale equations leads to more general two-phase flow models, the model used in this investigation is based on a multiphase extension of Darcy-Forchheimer's equations (Forchheimer (1901)) with a friction term, as suggested by the theoretical results. One of the particular features of the studied configuration is that a strong flow of steam is generated by quenching of the superheated particles. Under certain conditions, this steam flow is able to create a vertical pressure gradient which can lead the water in the more permeable medium to flow faster than the injection velocity. As a consequence, some of the injected water does not participate to the cooling of the central porous medium and the efficiency of cooling is reduced. This paper deals with the study of particle bed coolability in a damaged nuclear reactor core upon a loss of coolant accident, by water injection from the bottom (reflooding). This physical situation involves a strong evaporation of water in the particle bed, leading to high velocity flow of steam. It has been investigated by several authors until recently (Tutu et al. (1984), Atkhen and Berthoud (2003), Chikhi et al. (2015)).

The investigation is concerned in the two phase flow in a particle bed stratified vertically. It is a porous medium composed of two concentric cylindrical layers of contrasting thickness and permeability, the central one being less permeable and less porous. The analytical model is developed to predict the behavior of water in the lateral layer (bypass) of larger permeability and porosity representing the case of bottom reflooding of a hot debris bed surrounded by an intact zone in a degraded nuclear reactor core during an accidental scenario. The redistribution of water and steam into the bypass is investigated in several steps in order to evaluate the pressure gradient which can be generated downstream of the quench front. Considering a set of mass and energy balance equations, taken over frames of reference moving at the quench front velocity, allows estimating the water-to-steam conversion ratio and the quench front velocity. The velocity of water in the bypass, which is shown to be the unique solution of a system of two equations (mass conservation and momentum conservation) is then computed and consequently the flow rates of water and steam downstream. The results are then compared to PEARL bottom reflooding experimental tests (Chikhi et al. (2015)).

The presence of intact zones (bypass) surrounding a hot debris bed formed upon a severe accident in a nuclear reactor core lead to the significant diversion of the injected coolant flow, in the aim of achieving the cooling of the heat-accumulating hot debris bed, into the periphery provided it is highly permeable compared to the debris bed. It can extend the time required to achieve a total quenching of the hot debris bed questioning its coolability which also depends on the

initial thermal state of the bed. If for instance the formed debris bed resulting from a severe accident was being uncovered and heated up to high temperatures, the reflooding process in the presence of a highly permeable bypass could allow certain zones in the debris bed to continue further heating compromising its coolability as it could reach the melting point if the coolant didn't succeed to penetrate to that zone. It is therefore a major concern to investigate thoroughly the behavior of water entrainment in the bypass during the reflooding process in order to estimate the corresponding limitations and define the factors that describe the coolability of the debris bed.

Analytical model development - Two phase flow redistribution

Physical laws To investigate such a two-phase flow in a porous medium, an analytical model will be derived to describe the entrainment behavior of water into the bypass. The change of scale for Stokes flow equation and continuity has already been investigated leading to Darcy's law (Whitaker (1996)). The equations used to develop this model are based on Darcy's law (Darcy (1856)) with Forchheimer correction (Forchheimer (1901)) to include non-linear velocity terms. In a homogeneous medium, for a single phase θ , the Darcy-Forchheimer law relates the gradient of the intrinsic phase-averaged pressure $\nabla \langle p_\theta \rangle^\theta$, where p_θ is the pore-scale pressure field, to the average velocity (filtration velocity), $\langle \mathbf{v}_\theta \rangle$, where \mathbf{v}_θ is the pore-scale velocity field, as:

$$\langle \mathbf{v}_\theta \rangle = -\frac{\mathbf{K}}{\mu_\theta} \cdot (\nabla \langle p_\theta \rangle^\theta - \rho_\theta \mathbf{g}) - \mathbf{F}(\langle \mathbf{v}_\theta \rangle) \cdot \langle \mathbf{v}_\theta \rangle \quad (1)$$

where \mathbf{K} is the intrinsic permeability tensor of the medium, \mathbf{g} is the gravitational acceleration, $(p_\theta, \rho_\theta, \mu_\theta)$ are the pressure, density, and dynamic viscosity of the θ -phase, and \mathbf{F} is the Forchheimer correction tensor. Both tensors \mathbf{K} and \mathbf{F} are isotropic. A discussion on the estimation of the inertial contribution for particle debris beds can be found in Clavier (2015).

For a (liquid-gas) two-phase flow system, the equations obtained theoretically by Lasseux et al. (2008) have the following structure:

$$\langle \mathbf{v}_l \rangle = -\frac{\mathbf{K}_{ll}}{\mu_l} \cdot (\nabla \langle p_l \rangle^l - \rho_l \mathbf{g}) - \mathbf{F}_{ll} \cdot \langle \mathbf{v}_l \rangle + \mathbf{K}_{lg} \cdot \langle \mathbf{v}_g \rangle - \mathbf{F}_{lg} \cdot \langle \mathbf{v}_g \rangle \quad (2)$$

$$\langle \mathbf{v}_g \rangle = -\frac{\mathbf{K}_{gg}}{\mu_g} \cdot (\nabla \langle p_g \rangle^g - \rho_g \mathbf{g}) - \mathbf{F}_{gg} \cdot \langle \mathbf{v}_g \rangle + \mathbf{K}_{gl} \cdot \langle \mathbf{v}_l \rangle - \mathbf{F}_{gl} \cdot \langle \mathbf{v}_l \rangle \quad (3)$$

Tensors K_{ll} and K_{gg} represent the intrinsic viscous terms for each phase, whereas K_{lg} and K_{gl} are the viscous cross-terms. In quasi-static conditions, these tensors are independent of velocity of each phase but rather influenced and described by the void fraction, the geometry of the porous medium, and the structure of the flow at pore scale (Clavier (2015)). Tensors F_{ll} and F_{gg} represent the intrinsic inertial effects whereas F_{lg} and F_{gl} are the inertial cross-terms. They generally depend on the void fraction, the porous medium geometry and the structure of the flow at pore scale but also on the liquid and gas velocities $\langle \mathbf{v}_l \rangle$ and $\langle \mathbf{v}_g \rangle$.

To simplify the nomenclature, we introduce the notations:

$$\langle \mathbf{v}_\theta \rangle = U_\theta \quad (4)$$

$$\langle p_\theta \rangle^\theta = P_\theta \quad (5)$$

In the z -direction, the 1-D system of equations can be rather written for each phase in the general form:

$$-\partial P_g / \partial z = \rho_g g + a_g U_g + b_g U_g^2 + c_g U_g U_l + d_g U_l + e_g U_l^2 \quad (6)$$

$$-\partial P_l / \partial z = \rho_l g + a_l U_l + b_l U_l^2 + c_l U_l U_g + d_l U_g + e_l U_g^2 \quad (7)$$

In which the superficial velocity U_θ of the phase θ is related to the intrinsic average velocity $\langle \mathbf{v}_\theta \rangle^\theta$ in a porous medium of porosity ε by:

$$U_\theta = \varepsilon S_\theta \langle \mathbf{v}_\theta \rangle^\theta \quad (8)$$

with S_θ the θ -phase saturation.

The benefit of writing it in this general form is that it allows to embed any form of the pressure drop equation or any interfacial friction law, quadratic in the phases velocities, which is the case for the interfacial friction laws present in the literature (Tung and Dhir (1988), Schulenberg and Müller (1987), Schmidt (2007)).

If the tensors \mathbf{K} and \mathbf{F} are assumed diagonal ($\mathbf{K}_{ij}=0$, $\mathbf{F}_{ij}=0$ for $i \neq j$) by considering that the cross-terms in both tensors are null, then only the intrinsic inertial terms are included and it renders Ergun's law (Ergun (1952)) in the form:

$$-\frac{\partial P_\theta}{\partial z} = \rho_\theta g + \frac{\mu_\theta}{\kappa} U_\theta + \frac{\rho_\theta}{\eta} U_\theta^2 \quad (9)$$

where κ and η represent the intrinsic permeability and passability of the medium. The linear and quadratic velocity terms in the right hand side of Eq. 9 represents the viscous and kinetic energy losses per unit length respectively.

For spherical particles, combining this law with Kozeny-Carman equation Carman (1937), the permeability and passability are obtained correlated to the particles diameter d_p and the porosity ε of the bed as follows:

$$\kappa = \frac{\varepsilon^3 d_p^2}{180(1 - \varepsilon)^2} \quad \text{and} \quad \eta = \frac{\varepsilon^3 d_p}{1.75(1 - \varepsilon)} \quad (10)$$

For the two-phase flow in a porous medium, the Darcy-Forchheimer equation for each phase θ is written in a similar form as Eq. 9. It is further generalized to include the relative permeability κ_θ and the relative passability η_θ which have been determined for spherical particles according to different correlations. A widely used and rather classical relations for a two-phase (liquid-gas) system was proposed by Brooks and Corey (1966) to define relative permeability and relative passability of each phase as follows:

$$\kappa_l = (1 - \alpha)^{n\kappa} \quad \text{and} \quad \eta_l = (1 - \alpha)^{n\eta} \quad (11)$$

$$\kappa_g = \alpha^{n\kappa} \quad \text{and} \quad \eta_g = \alpha^{n\eta} \quad (12)$$

where $\alpha = S_g$ is the void fraction and the subscripts (l, g) refer to the phases (liquid, gas).

This classical formulation was cited many times in the literature by several authors (Lipinski (1984), Reed (1982) and Hu and Theofanous (1991)) who proposed different sets of the exponents $n\kappa$ and $n\eta$. A different formulation was later proposed by Fourar and Lenormand (2000) in which

the relative permeability is equal to the relative passability for the same fluid phase and where the gas phase relative permeability and passability not only depended on the void fraction but also on the viscosities of liquid and gas.

The generalized Darcy Forchheimer momentum equations (including Forchheimer correction factors but no cross-terms) for the two-phase (liquid, gas) system are written as:

$$-\frac{\partial P_g}{\partial z} = \rho_g g + \frac{\mu_g}{\kappa \kappa_g} U_g + \frac{\rho_g}{\eta \eta_g} U_g^2 \quad (13)$$

$$-\frac{\partial P_l}{\partial z} = \rho_l g + \frac{\mu_l}{\kappa \kappa_l} U_l + \frac{\rho_l}{\eta \eta_l} U_l^2 \quad (14)$$

However, adding an interfacial friction law to the momentum equations introduces some cross-terms. A convenient law that is often used in thermal-hydraulics codes to study this type of flow in porous media is the Schulenberg-Muller law (Schulenberg and Müller (1984)). The authors correlated their data based on experimental results of debris bed bottom reflooding tests and deduced an equation for the interfacial friction from the measured pressure drop in the bed. It will be considered in this study to produce the results and it is defined as follows:

$$-\frac{\partial P_g}{\partial z} = \rho_g g + \frac{\mu_g}{\kappa \kappa_g} U_g + \frac{\rho_g}{\eta \eta_g} U_g^2 + \frac{F_i}{\alpha} \quad (15)$$

$$-\frac{\partial P_l}{\partial z} = \rho_l g + \frac{\mu_l}{\kappa \kappa_l} U_l + \frac{\rho_l}{\eta \eta_l} U_l^2 - \frac{F_i}{1 - \alpha} \quad (16)$$

where F_i represents the interfacial drag force defined by:

$$F_i = 350 (1 - \alpha)^7 \alpha \frac{\rho_l K}{\eta \sigma} (\rho_l - \rho_g) g \left(\frac{U_g}{\alpha} - \frac{U_l}{1 - \alpha} \right)^2 \quad (17)$$

with σ being the surface tension. They adopted Brooks and Correy relations (Brooks and Corey (1966)) for the liquid phase relative permeability and passability with:

$$\kappa_l = (1 - \alpha)^3 \quad \text{and} \quad \eta_l = (1 - \alpha)^5 \quad (18)$$

whereas for the gas phase, they assumed a relative permeability of $\kappa_g = \alpha^3$ and deduced the corresponding relative passability η_g to be:

$$\eta_g = 0.1 \alpha^4 : \alpha \leq 0.3 \quad \text{and} \quad \alpha^6 : \alpha > 0.3 \quad (19)$$

Inlet Velocity The development of the analytical model starts by writing the mass and energy balance equation for the fluid and the solid particles, in a frame of reference moving with the quench front velocity v^{qf} , between the elevations (z_0, z_1) and (z_1, z_2) . They correspond to the quench front level, start of two-phase zone and the end of the two phase zone respectively as shown in Figure 1.

First, water is injected into the system from bottom and moves upwards. Below the quench front

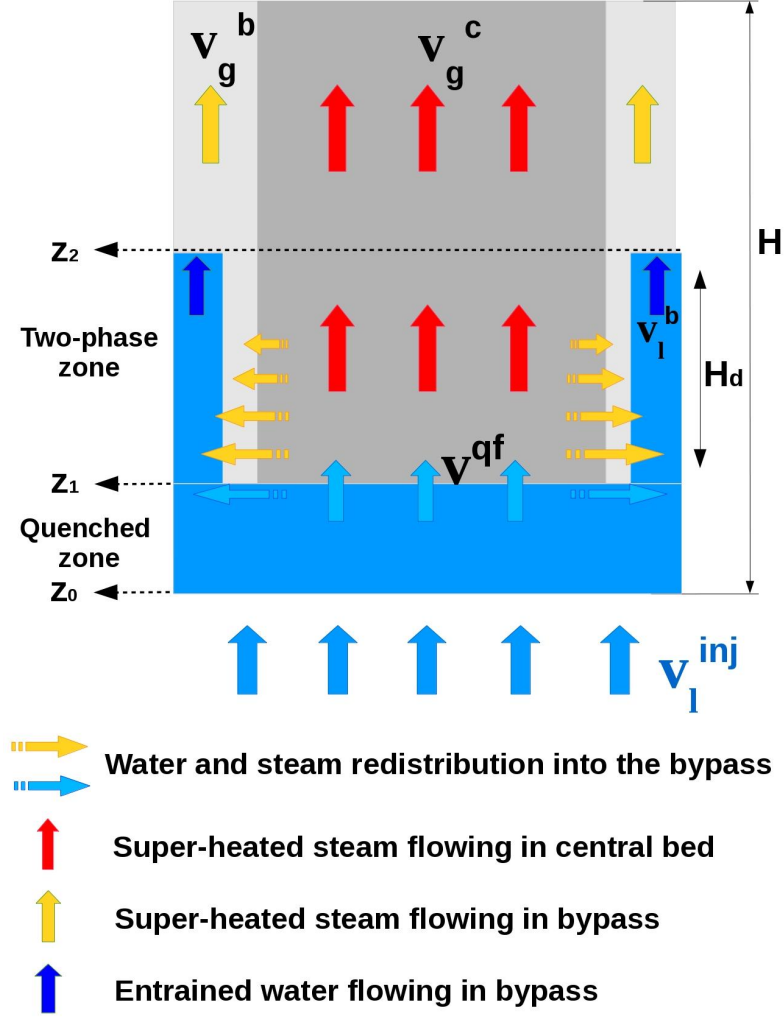


Figure 1: Two phase flow redistribution

level, the flow is assumed purely liquid and, for a given elevation, the pressure in the center is approximately equal to that in the bypass, so we can write:

$$\frac{\partial P_l^c}{\partial z} \approx \frac{\partial P_l^b}{\partial z} \quad (20)$$

The Reynold's number for this flow in the central porous layer is:

$$Re_l^c = \frac{\rho_l v_l^{inj} d_p^c}{\mu_l (1 - \varepsilon^c)} \quad (21)$$

For an injection velocity $v_l^{inj}=1.388 \times 10^{-3}$ m/s, $Re^c=24.3$, and for the bypass zone $Re^b=48.6$. Hence, the inertial terms should be included. Eq. 20 is thus expanded using the single-phase Darcy-Forchheimer equation as defined by Eq. 9:

$$-\rho_l g - \frac{\mu_l}{\kappa^c} U_l^{cin} - \frac{\rho_l}{\eta^c} (U_l^{cin})^2 = -\rho_l g - \frac{\mu_l}{\kappa^b} U_l^{bin} - \frac{\rho_l}{\eta^b} (U_l^{bin})^2 \quad (22)$$

thus arriving at a quadratic equation relating U_l^{cin} and U_l^{bin} .

On the other hand, writing the mass balance equation between the injection level and this level, we obtain:

$$\varepsilon^c S^c \rho_l v_l^{c\,in} + \varepsilon^b S^b \rho_l v_l^{b\,in} = \varepsilon^0 (S^b + S^c) \rho_l v_l^{inj} \quad (23)$$

with

$$U_l^{c\,in} = \varepsilon^c v_l^{c\,in} \quad \text{and} \quad U_l^{b\,in} = \varepsilon^b v_l^{b\,in} \quad (24)$$

Substituting Eq. 23 into the quadratic Eq. 22, we can then explicitly relate each of $v_l^{b\,in}$ and $v_l^{c\,in}$ to the injection velocity v_l^{inj} .

Quench Front Velocity The quasi static propagation of the quench front is assumed upon the observations made in the PEARL experiments where the quench front velocity was quasi-constant as well as the steam production rate (Chikhi et al. (2015)). However, some other dynamic processes occur fastly in the beds and they are regarded as transient effects corresponding to: (1) the arrival of the quench front at the bottom superheated debris bed and (2) its exit at the top of the debris bed at the last phase of the quenching process. The quasi-constant steam production rate during reflooding a superheated debris bed was also observed by Tutu et al. (1984) and Tung and Dhir (1983).

We Proceed by writing the mass balance equation for the fluid between elevations z_1 and z_2 in a relative frame of reference moving at the quench front velocity v^{qf} :

$$\begin{aligned} & \alpha_1^c \varepsilon^c S^c \rho_g (v_{g1}^c - v^{qf}) + (1 - \alpha_1^c) \varepsilon^c S^c \rho_l (v_{l1}^c - v^{qf}) + (1 - \alpha_1^b) \varepsilon^b S^b \rho_l (v_{l1}^b - v^{qf}) \\ & = \alpha_2^c \varepsilon^c S^c \rho_g (v_{g2}^c - v^{qf}) + \alpha_2^b \varepsilon^b S^b \rho_g (v_{g2}^b - v^{qf}) \end{aligned} \quad (25)$$

in which the subscripts 1 and 2 refer to the elevations z_1 and z_2 respectively, with $\alpha_2^c = \alpha_2^b = 1$ (exiting as pure steam), and $\alpha_1^b = 0$ (only liquid enters into the bypass at the quench front level).

Then writing the energy balance equation between elevations z_1 and z_2 in a frame of reference moving at the quench front velocity v^{qf} , with the saturation temperature $T_{sat} = 273K$ as a reference temperature:

$$\begin{aligned} & \alpha_1^c \varepsilon^c S^c \rho_g (v_{g1}^c - v^{qf}) h_g^{sat} + (1 - \alpha_1^c) \varepsilon^c S^c \rho_l (v_{l1}^c - v^{qf}) h_l^{sat} + \varepsilon^b S^b \rho_l (v_{l1}^b - v^{qf}) c_{pl} \Delta T_l^b \\ & = (1 - \varepsilon^c) S^c \rho_s (v_{s2}^c - v^{qf}) c_{ps} \Delta T_s^c + (1 - \varepsilon^b) S^b \rho_s (v_{s2}^b - v^{qf}) c_{ps} \Delta T_s^b \\ & \alpha_2^c \varepsilon^c S^c \rho_g (v_{g2}^c - v^{qf}) (h_g^{sat} + c_{pg} \Delta T_g^c) + \alpha_2^b \varepsilon^b S^b \rho_g (v_{g2}^b - v^{qf}) (h_g^{sat} + c_{pg} \Delta T_g^b) \end{aligned} \quad (26)$$

with $v_{s2}^b = v_{s2}^c = 0$ (fixed solid), and assuming that the superheated steam exits at the same temperature from the center and the bypass ($\Delta T_g^c = \Delta T_g^b = \Delta T_g$). Eq. 26 can be reformed and written as:

$$\begin{aligned} & [\varepsilon^c S^c \rho_g (v_{g2}^c - v^{qf}) + \varepsilon^b S^b \rho_g (v_{g2}^b - v^{qf})] (h_g^{sat} + c_{pg} \Delta T_g) \\ & = \alpha_1^c \varepsilon^c S^c \rho_g (v_{g1}^c - v^{qf}) h_g^{sat} + (1 - \alpha_1^c) \varepsilon^c S^c \rho_l (v_{l1}^c - v^{qf}) h_l^{sat} \\ & + \varepsilon^b S^b \rho_l (v_{l1}^b - v^{qf}) c_{pl} \Delta T_l^b + (1 - \varepsilon^c) S^c \rho_s v^{qf} c_{ps} \Delta T_s^c + (1 - \varepsilon^b) S^b \rho_s v^{qf} c_{ps} \Delta T_s^b \end{aligned} \quad (27)$$

Substituting Eq. 25 into Eq. 27 to eliminate the terms referring to elevation z_2 and regrouping the terms associated to v^{qf} , we get:

$$\begin{aligned}
& v^{qf} \{ \alpha_1^c \varepsilon^c S^c \rho_g c_{pg} \Delta T_g + (1 - \alpha_1^c) \varepsilon^c S^c \rho_l (\Delta h^{sat} + c_{pg} \Delta T_g) \\
& + \rho_s c_{ps} [(1 - \varepsilon^c) S^c \Delta T_s^c + (1 - \varepsilon^b) S^b \Delta T_s^b] + \varepsilon^b S^b \rho_l (h_g^{sat} + c_{pg} \Delta T_g - c_{pl} \Delta T_l^b) \} \\
& = \varepsilon^b S^b \rho_l v_{l1}^b (h_g^{sat} + c_{pg} \Delta T_g - c_{pl} \Delta T_l^b) + \alpha_1^c \varepsilon^c S^c \rho_g v_{g1}^c c_{pg} \Delta T_g \\
& + (1 - \alpha_1^c) \varepsilon^c S^c \rho_l v_{l1}^c (\Delta h^{sat} + c_{pg} \Delta T_g)
\end{aligned} \tag{28}$$

Now, for the fluid at the bottom (between z_0 and z_1), writing the mass balance equation, we get:

$$\alpha_1^c \varepsilon^c S^c \rho_g v_{g1}^c + (1 - \alpha_1^c) \varepsilon^c S^c \rho_l v_{l1}^c + \varepsilon^b S^b \rho_l v_{l1}^b = \varepsilon^0 \rho_l (S^b + S^c) v_l^{inj} \tag{29}$$

In quench front velocity formulation (Eq. 28), knowing that the first term of the right-hand-side can be written in the form:

$$\varepsilon^b S^b \rho_l v_{l1}^b (h_g^{sat} + c_{pg} \Delta T_g) = \varepsilon^b S^b \rho_l v_{l1}^b (\Delta h^{sat} + c_{pg} \Delta T_g) + \varepsilon^b S^b \rho_l v_{l1}^b h_l^{sat} \tag{30}$$

Then Eq. 28 can be written as:

$$\boxed{v^{qf} = \frac{F}{E} = \frac{F_1 + F_2 + F_3}{E_1 + E_2 + E_3 + E_4}} \tag{31}$$

F [J/s] and E [J/m] terms are listed in the Appendix A.1.

The ratio of the quench front velocity v^{qf} to the injection velocity v^{inj} is defined by γ_u :

$$\gamma_u = \frac{v^{qf}}{v_l^{inj}} = \frac{F}{v_l^{inj} E} \tag{32}$$

Water-to-Steam Conversion During reflooding the superheated debris bed with a constant injection rate, the injected water evaporates and steam is produced and collected downstream the beds. In the analysis of reflooding a homogeneous superheated debris bed, (Tutu et al. (1984)) and (Tung and Dhir (1983)) had proposed a formulation of the water-to-steam conversion rate. Chikhi et al. (2015) have later proposed an updated formulation taking into account two specific features of the PEARL experiment which are relevant to the formed debris bed in a damaged reactor core. Following a similar approach, this model is developed to take into account the presence of a lateral (layer bypass) of larger permeability surrounding the central debris bed.

The ratio of the steam production rate to the water injection rate is called the water-to-steam conversion rate γ_{cr} . It is regarded as a measure of the efficiency of reflooding and defined by:

$$\gamma_{cr} = \frac{\phi_g^{out}}{\phi_l^{inj}} \tag{33}$$

Having estimated the quench front velocity v^{qf} obtained upon computing γ_u , we attempt to derive a formulation for the water-to-steam conversion ratio which relates the mass flow rate of steam produced at the outlet to the injected water flow rate by Eq. 33 where:

$$\phi_g^{out} = \varepsilon^c S^c \rho_g v_{g2} + \varepsilon^b S^b \rho_g v_{g2}^b \quad (34)$$

is determined by Eq. 25 by:

$$\begin{aligned} \varepsilon^c S^c \rho_g v_{g2}^c + \varepsilon^b S^b \rho_g v_{g2}^b &= \alpha_1^c \varepsilon^c S^c \rho_g (v_{g1}^c - v^{qf}) + (1 - \alpha_1^c) \varepsilon^c S^c \rho_l (v_{l1}^c - v^{qf}) \\ &+ \varepsilon^b S^b \rho_l (v_{l1}^b - v^{qf}) + (\varepsilon^c S^c \rho_g + \varepsilon^b S^b \rho_g) v^{qf} \end{aligned} \quad (35)$$

Regrouping the terms associated to v^{qf} and substituting the other velocity terms using Eq. 29, we obtain:

$$\begin{aligned} \phi_g^{out} &= \varepsilon^0 \rho_l (S^b + S^c) v_l^{inj} - v^{qf} [\alpha_1^c \varepsilon^c S^c \rho_g + (1 - \alpha_1^c) \varepsilon^c S^c \rho_l \\ &+ \varepsilon^b S^b \rho_l - (\varepsilon^c S^c \rho_g + \varepsilon^b S^b \rho_g)] \end{aligned} \quad (36)$$

or more simply

$$\phi_g^{out} = \varepsilon^0 \rho_l (S^b + S^c) v_l^{inj} - v^{qf} (\rho_l - \rho_g) (\varepsilon^b S^b + \varepsilon^c S^c - \alpha_1^c \varepsilon^c S^c) \quad (37)$$

by definition the conversion rate is given by:

$$\gamma_{cr} = \frac{\phi_g^{out}}{\phi_l^{inj}} = \frac{\phi_g^{out}}{\varepsilon^0 \rho_l (S^b + S^c) v_l^{inj}} \quad (38)$$

Therefore, the derived water-to-steam conversion rate γ_{cr} is given by:

$$\gamma_{cr} = 1 - \gamma_u \left[\left(1 - \frac{\rho_g}{\rho_l} \right) \left(\frac{\varepsilon^b S^b + \varepsilon^c S^c}{\varepsilon^0 S} - \frac{\varepsilon^c S^c \alpha_1^c}{\varepsilon^0 S} \right) \right] \quad (39)$$

Defining the relative cross-sectional surface ratio of the central bed to the total surface by ψ :

$$\psi = \frac{S^c}{S} = \frac{S^c}{S^c + S^b} \quad (40)$$

We can then simply write:

$$\boxed{\gamma_{cr} = 1 - \frac{\gamma_u}{\varepsilon^0} \left[\left(1 - \frac{\rho_g}{\rho_l} \right) (\varepsilon^b (1 - \psi) + \varepsilon^c \psi (1 - \alpha_1^c)) \right]} \quad (41)$$

where

$$\gamma_u = \frac{v^{qf}}{v_l^{inj}} \quad (42)$$

S is the total cross-sectional surface, v_l^{inj} is the water injection velocity and v^{qf} is the velocity of the quench front which is assumed quasi-static.

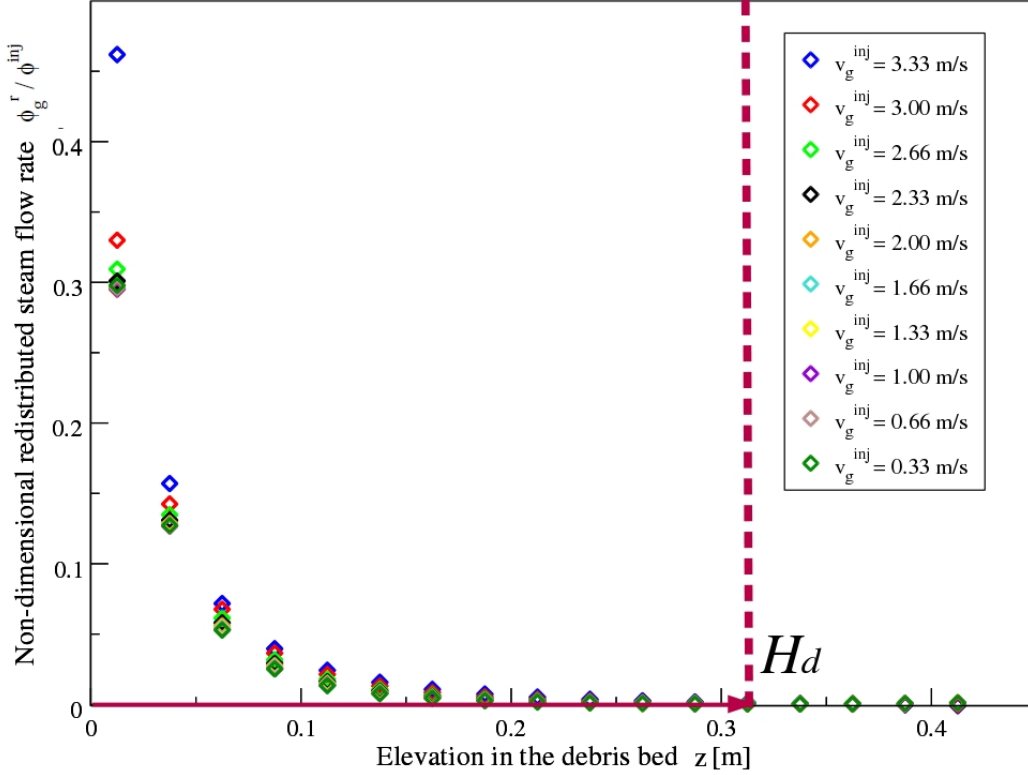


Figure 2: Single phase flow simulation - Steam redistribution into the bypass for different injection velocities

Entrainment Velocity of Water Upon water injection and evaporation, steam produced at the quench front level is redistributed radially into the bypass. Single phase steam flow simulations showed that for different injection flow rates, there exists a length H_d over which this redistribution occurs (Figure 2). This length H_d is approximately the same for different flow rates, it corresponds to the elevation z_2 above the quench front level and above which no more steam or water is redirected radially into the bypass.

$$\phi_g^{r \rightarrow b}(z = H_d) \approx 0 \quad (43)$$

where $\phi_g^{r \rightarrow b}(z)$ represent the integral steam flux redistributed radially, from the central layer to the bypass, up to an elevation z .

At this level, the pressure in the center is approximately equal to that in the bypass. This allows writing an equality of the vertical pressure gradients for the gas phase in the center and the bypass:

$$\frac{\partial P_g^c}{\partial z} \approx \frac{\partial P_g^b}{\partial z} \quad (44)$$

Expanding this equality using the Darcy-Forchheimer equation (Eq. 9) renders a quadratic equations relating the gas phase velocities in the center and the bypass by:

$$\rho_g g + \frac{\mu_g}{\kappa^c} U_g^c + \frac{\rho_g}{\eta^c} (U_g^c)^2 = \rho_g g + \frac{\mu_g}{\kappa^b} U_g^b + \frac{\rho_g}{\eta^b} (U_g^b)^2 \quad (45)$$

Then relating the flow rate of steam produced to the water injection flow rate, as defined earlier by the conversion rate equation (Eq. 33):

$$\gamma_{cr} \rho_l S v_l^{inj} = \rho_g S v_g^{out} \quad (46)$$

$$\gamma_{cr} \rho_l S v_l^{inj} = \alpha^b \rho_g \varepsilon^b S^b v_g^b + \alpha^c \rho_g \varepsilon^c S^c v_g^c \quad (47)$$

At this level, it is pure steam exiting the center ($\alpha^c=1$) at the top of the two-phase zone. Eq. 47 is then reformed to relate v_g^c , v_g^b , and v_l^{inj} by the following equation:

$$v_g^c = \frac{\psi \alpha^b \varepsilon^b}{\varepsilon^c (\psi - 1)} v_g^b + \frac{\gamma_{cr} \rho_l}{\rho_g \varepsilon^c (1 - \psi)} (v_l^{inj}) \quad (48)$$

Combining Eq. 48 and Eq. 45 reduces to a quadratic equation in v_g^b of the form:

$$(v_g^b)^2 + r_1 v_g^b + s_1 = 0 \quad (49)$$

This allows determining the steam velocities v_g^b and v_g^c in terms of the injection velocity v_l^{inj} and the system parameters.

Neglecting the capillary effects in the bypass (see Appendix A.2), the pressure of the gas phase can be assumed equal to that of the liquid phase and thus the following equation holds in the bypass:

$$\frac{\partial P_g^b}{\partial z} \approx \frac{\partial P_l^b}{\partial z} \quad (50)$$

Expanding it using Darcy-Forchheimer equations for two-phase flow written in the general form:

$$\rho_g g + a_g U_g + b_g U_g^2 + c_g U_g U_l + d_g U_l + e_g U_l^2 = \rho_l g + a_l U_l + b_l U_l^2 + c_l U_l U_g + d_l U_g + e_l U_g^2 \quad (51)$$

arrives a quadratic equation in v_l^b (velocity of water in the bypass), it has the form:

$$(v_l^b)^2 - m_l v_l^b + n_l = 0 \quad (52)$$

in which

$$m_l = \frac{(c_g - c_l) v_g + d_g - a_l}{b_l - e_g} \quad n_l = \frac{(\rho^l - \rho^g) g + v_g (d_l - a_g) + v_g^2 (e_l - b_g)}{b_l - e_g} \quad (53)$$

The solution $v_l^b(\alpha)$ for Eq. 52 is the first solution relating the velocity of the entrained water into the bypass v_l^b to the steam velocity and physical properties of the medium and the flow, it is given by:

$$\boxed{v_l^b(\alpha) = +\frac{1}{2} m_l \left[1 \pm \sqrt{1 - 4 \frac{n_l}{m_l^2}} \right]} \quad (54)$$

Written in this general form, Eq. 51 enables testing of any proposed variation in the momentum equations and assessing the sensitivity of the solutions to its terms.

The PEARL tests experimental results obtained at IRSN (Chikhi et al. (2015)) were considered for comparison. The main characteristics of those tests are listed in Table 1. Adopting the same configuration, the total height of the debris bed is $H=0.5$ m, the radius of the central bed is $R^c=0.225$ m whereas the more permeable bypass had a radial thickness of 0.045 m making the total radius of the system $R^{ext}=0.27$ m. The diameter of the particles in the center is $d_p^c=4$ mm whereas the more permeable bypass was composed of particles of larger diameter $d_p^b=8$ mm.

Table 1: PEARL Tests

Test number	Initial temperature (degC)	Injection velocity (m/h)	Pressure (bar)	Flooding mode
PA0	150	5	1	Bottom
PA1	400	5	1	Bottom
PA2	700	5	1	Bottom
P22	700	5	2	Bottom
PA4	400	2	1	Bottom
PA5	400	10	1	Bottom

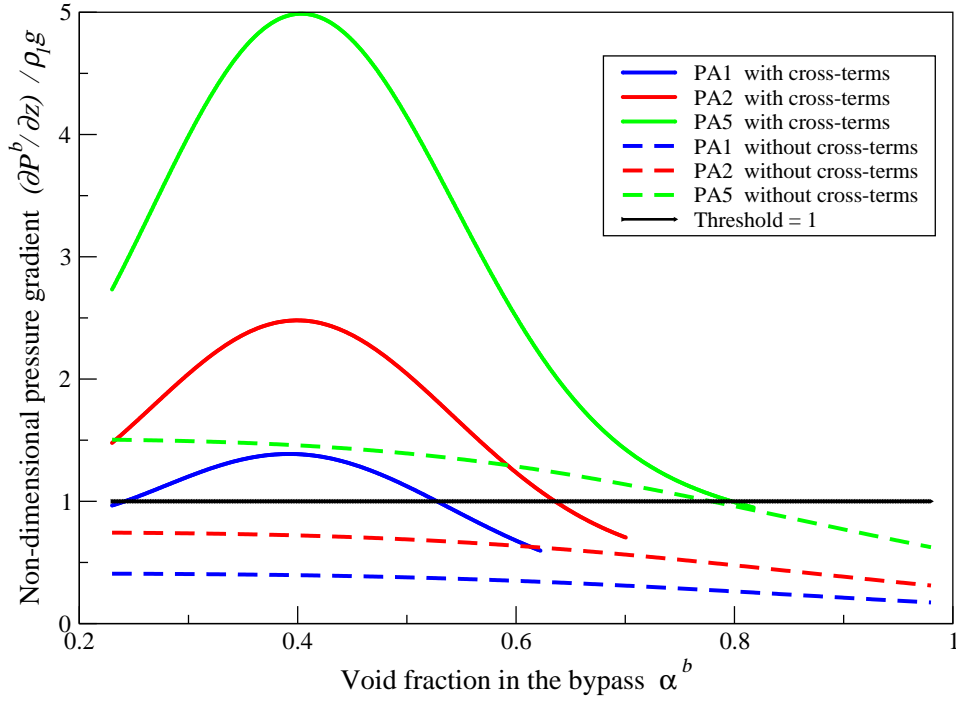


Figure 3: Non-dimensional vertical pressure gradient in bypass as function of void fraction α^b

For water to get entrained and advance in the bypass (i.e. obtaining non-zero solutions for v_l^b), the vertical pressure gradient must be larger than the hydrostatic pressure. The necessary condition for the entrainment of water in the bypass is defined by a threshold represented by the non-dimensional vertical pressure gradient in the bypass ω (Figure 3):

$$\omega = [\frac{\partial P_g^b}{\partial z}]/[\rho_l g] \quad (55)$$

The threshold is $\omega=1$. Below this threshold the entrainment of water in the bypass is impossible and the advance of water in the bypass is limited to the quench front velocity. The dashed lines correspond to the Generalized Darcy form of the momentum equations (i.e. no cross-terms, $\mathbf{K}_{ij}=0$, $\mathbf{F}_{ij}=0$ for $i \neq j$) whereas solid lines correspond to the Darcy-Forchheimer momentum equations (including cross-terms \mathbf{K}_{ij} , \mathbf{F}_{ij}). Entrainment occurs when the velocity of water in the bypass is significantly higher than the latter; with a least ratio $U_l^b/U^{qf} > 1.5$ which corresponds to the situations where the pressure gradient is sufficiently larger than the hydrostatic pressure.

For instance, considering three PEARL tests (PA1, PA2, and PA5) with different injection velocities. The quench front velocity and the conversion rate were obtained by the analytical model and the results of the modeled water velocity in the bypass $v_l^b(\alpha)$ provided by Eq. 54 (1st solution) are presented in Figure 4. It shows the occurrence of water entrainment in the bypass in all cases as demonstrated by the experiments with a 2-D shaped quench front propagation.

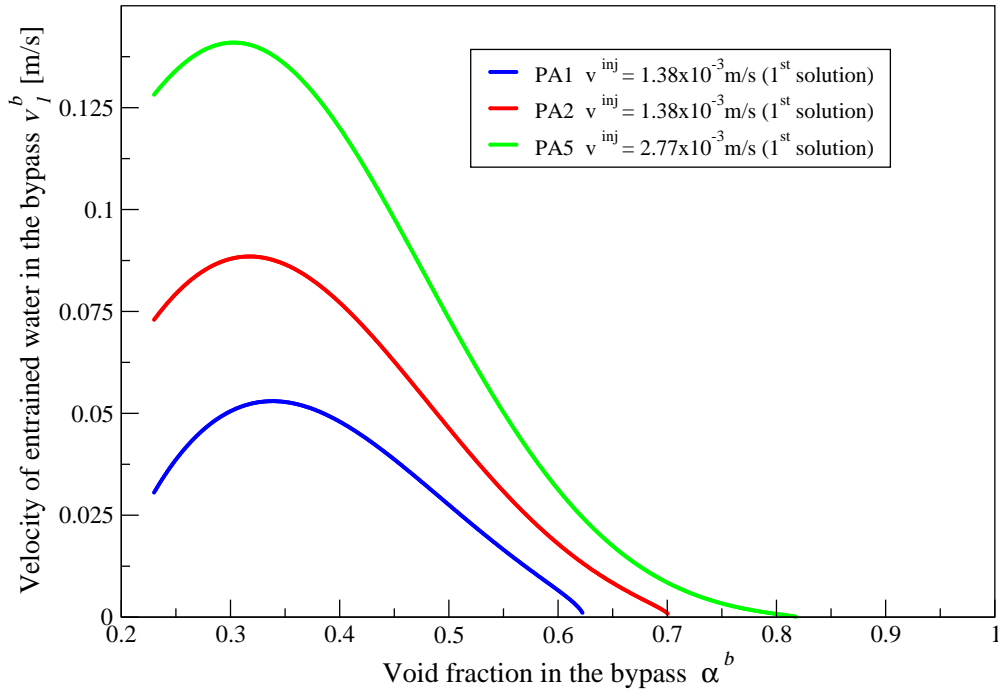


Figure 4: Entrained water velocity as function of void fraction $v_l^b(\alpha)$ for different PEARL tests - 1st solution

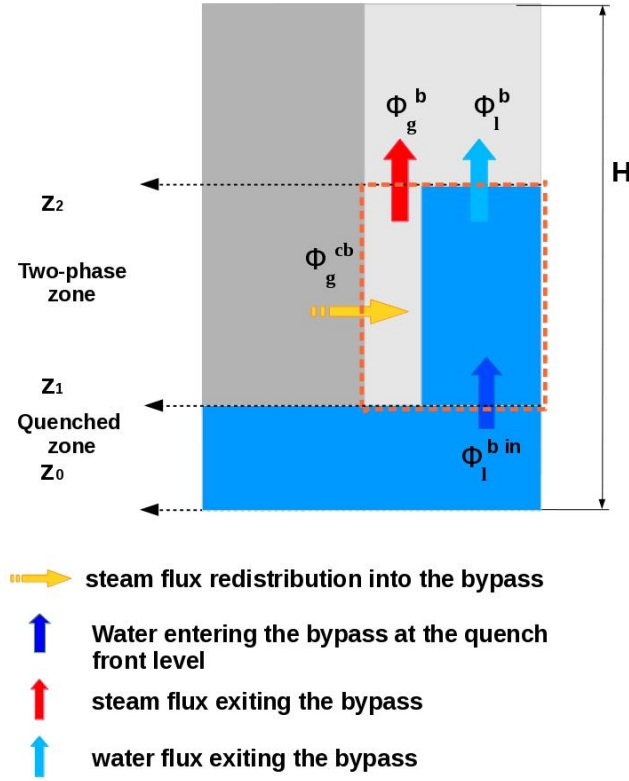


Figure 5: Mass balance in the bypass

Alternatively, the velocity of the entrained water is estimated by writing the mass balance equation over a control volume in the bypass between the quench front level z_1 and the top of the redistribution level z_2 as demonstrated in Figure 5. The mass balance over the orange contour writes:

$$\sum \phi_{in} = \sum \phi_{out} \quad (56)$$

$$\phi_l^{b in} + \phi_g^{cb} = \phi_l^b + \phi_g^b \quad (57)$$

with

$$\phi_g^{cb} = \phi_g^b \quad (58)$$

$$\phi_l^b = (1 - \alpha^b) \rho_l \varepsilon^b S^b (v_l^b - v^{qf}) \quad (59)$$

$$\phi_l^{b in} = \rho_l \varepsilon^b S^b (v_l^{b in} - v^{qf}) \quad (60)$$

where $v_l^{b in}$ is previously calculated by Eq. 23.

This provides another estimation of the water velocity in the bypass in terms of the void fraction α^b , injection velocity v_l^{inj} and the quench front velocity v^{qf} , defined by:

$$v_l^b = \frac{(v_l^{b in} - \alpha^b v^{qf})}{1 - \alpha^b} \quad (61)$$

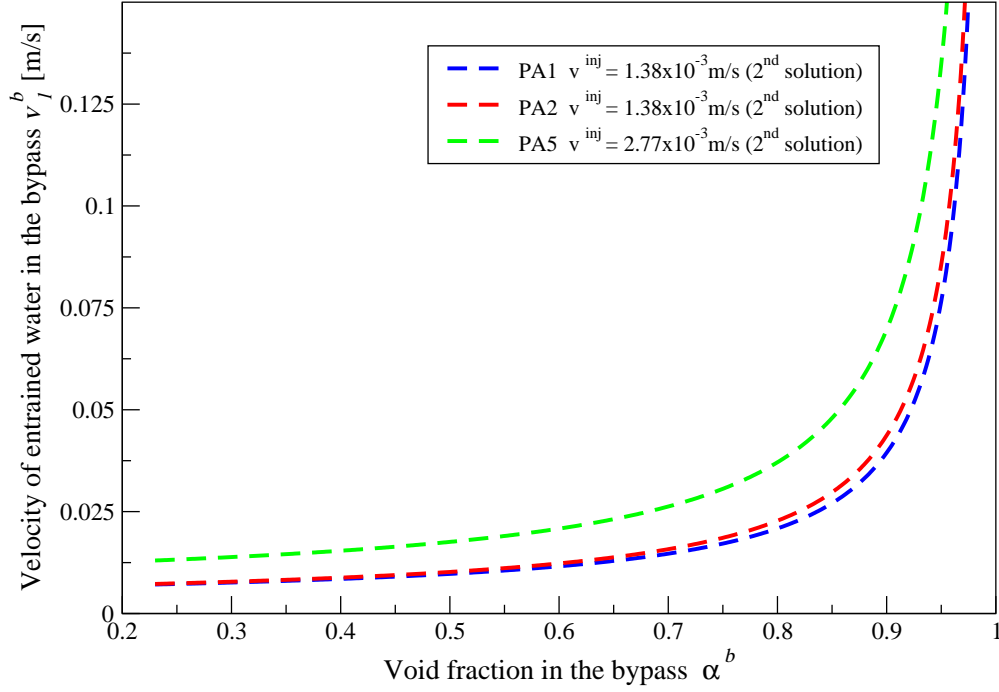


Figure 6: Entrained water velocity as function of void fraction $v_l^b(\alpha)$ for different PEARL tests - 2nd solution

This is a second solution for the velocity of entrained water in bypass $v_l^b(\alpha)$. It is presented in Figure 6 as function of the void fraction. An overlay of the two modeled solutions of $v_l^b(\alpha)$ provided by Eq. 54 and Eq. 61 presented in Figure 7 shows that the respective curves intersect at particular solutions whose abscissa α_i (Figure 8) are the void fractions in the bypass corresponding to each case, depending on the system characteristics and flow conditions.

However, instead of following this methodology of finding the intersect of two solutions for $v_l^b(\alpha)$, Newton-Raphson method could be applied to solve the same system of equations. In the latter case, we will only obtain the particular solution as a scalar output instead of profiles function of the void fraction, and problems while attempting convergence could also rise. The considered methodology provides a more clear view and helps to identify the behavior of the solutions and its sensitivity to the different input parameters.

Comparison against Experimental Results For the considered cases, the occurrence of water entrainment in the bypass was demonstrated by the condition $U_l^b/U^{qf} > 4$. This is consistent with the observations made upon the reflooding test where a 2-D shaped ($U_l^b > U^{qf}$) quench front propagation was obtained.

Table 2 compares the modeled results to the experimental results obtained for the considered PEARL tests. v^{qfc} and v^{qfb} are the measured quench front velocities in the center and the bypass. The modeled quench front velocity is comparable to that measured experimentally in the central

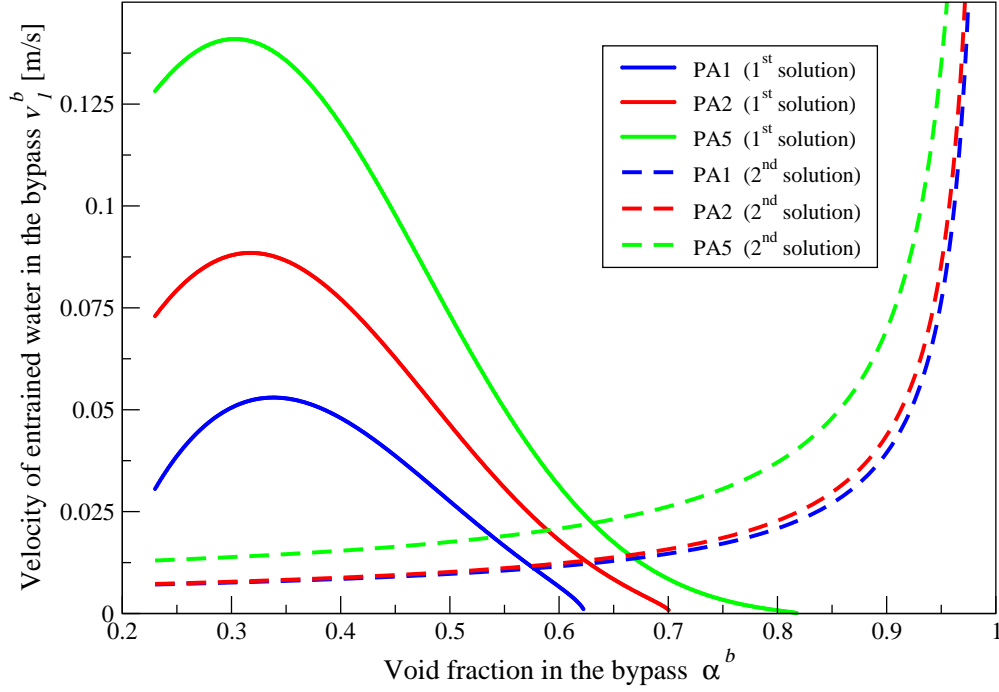


Figure 7: Velocity of entrained water in the bypass v_l^b as function of void fraction α^b for different PEARL tests - (intersect of solutions)

Table 2: Comparison of the Analytical Model Against Experimental Results for Different PEARL Tests; velocities unit=(mm/s)

Test	Porous medium	Experiment		Analytical model	
	v_l^{inj}	v_{qfb}	v_{qfc}	v_l^b	v_{qf}
PA1	3.472	7.3	2.17	13.10	2.20
PA2	3.472	14.2	1.00	16.10	1.62
P22	3.472	7.19	1.42	14.00	1.74
PA5	6.944	19.0	2.51	30.80	3.20
PA4	1.388	1.25	1.04	0.98	0.98

bed. In the bypass, the estimated velocity of the entrained water surpasses the quench front velocity for two main reasons; the analytical model estimates the water velocity which is generally faster than the quench front and there is also some uncertainty over the measurement of quench front velocity in the 4.5 cm thick bypass by a single thermocouple in the radial direction. Furthermore, the model succeeded to predict the entrainment of water in the bypass in all the cases (PA1, PA2, P22, and PA5) in which water advances in the bypass at velocities higher than the quench front velocity. However, the results obtained without the interfacial friction terms (i.e. using Generalized Darcy-Forchheimer law with all cross-terms K_{lg} , K_{gl} , F_{lg} , and F_{gl} set null) couldn't predict

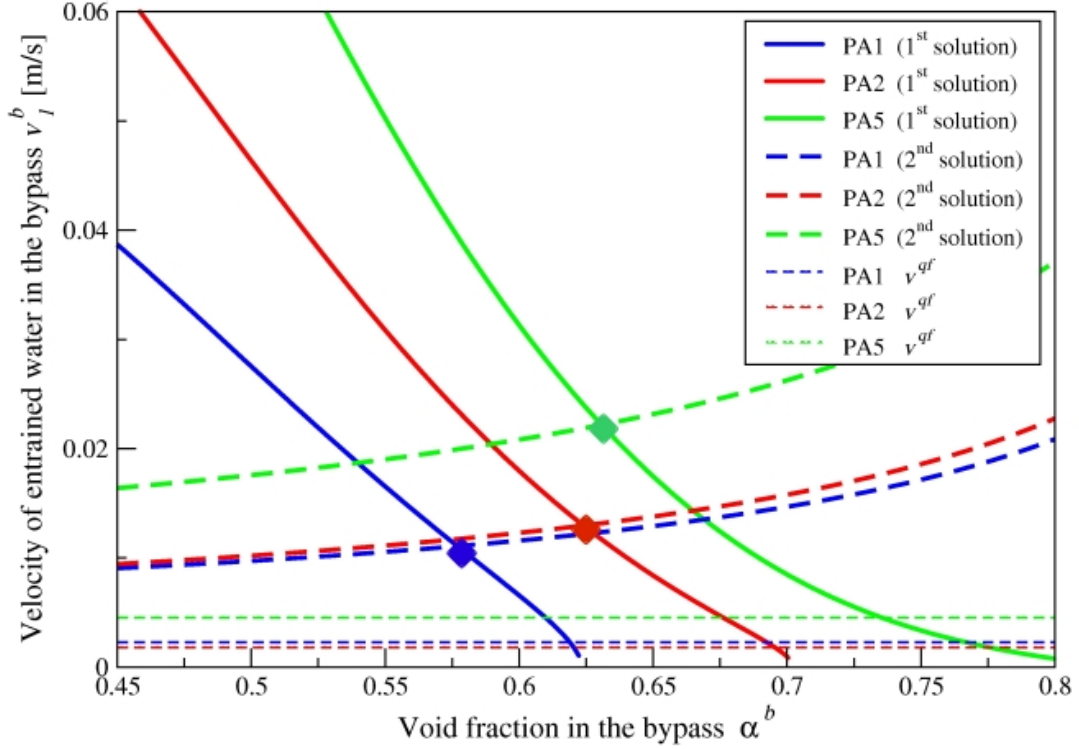


Figure 8: Intersection of bypass water velocity curves at the particular solution at abscissa α_i - (Solutions intersect, Zoom-in)

well the entrainment behavior. This is due to the fact that the considered cases correspond to the limiting geometric and flow conditions for which the predefined threshold for entrainment occurrence is compromised. Excluding the cross-terms from the momentum equations underestimated the vertical pressure gradient in the bypass in some cases (insufficient for entrainment, see Figure 3). For higher injection flow rates, the entrainment could be predicted. Yet, including non-zero cross-terms is necessary to obtain good estimations.

Conclusion

In this study, an investigation of two-phase (water and steam) flow in a heated porous medium composed of two cylindrical layers of contrasting porosity and permeability was conducted. An analytical two-phase model was derived to describe the entrainment behavior of water into the bypass. The criterion for which the entrained water progresses in the bypass faster than the quench front velocity has been examined for different cases. The velocity of the entrained water in bypass was estimated analytically as well as the void fraction in the bypass for the corresponding system configuration and flow conditions.

This simplified analytical model forms a tool to perform fast calculations of two phase flow redistribution in such a porous layers system, with different thickness, porosity and permeability and assess the conditions for water entrainment. It also allows testing different correlations in the vari-

ations of the momentum equations for porous media such as relative permeability and passability correlations, interfacial friction laws ...

The model provides good qualitative and quantitative results for two-phase flow redistribution downstream of the quench front as compared to the results obtained in PEARL reflooding tests where it predicts the occurrence of entrainment (advance of water in the bypass at a velocity v_l^b higher than the quench front velocity v^{qf}) and a comparable water velocity in all the cases.

The developed model has several advantages. It is written in a rather general form including the Forchheimer correction terms and non-zero cross-terms in the generalized Darcy-Forchheimer momentum equation. It allows to test easily and efficiently any proposed variation of the momentum equation including changes in correlations and friction laws up to quadratic terms. The model allows performing fast evaluations of the efficiency of cooling by computing the fraction of the injected flow rate that participates in cooling. Upscaling to the reactor scale is straightforward, provided the geometry and boundary conditions are respected. Thus the model is very useful to estimate the total quenching time and the maximum temperature that could be reached by the hot debris bed at large scales in accidental conditions. It can be also used to perform sensitivity studies on the physical properties of the particle beds and the fluid, as well as different variations of the momentum equations. For instance, it was shown that the Generalized Darcy law is not able to provide acceptable evaluations whereas considering non-zero cross-terms in the Darcy Forchheimer equation by including an interfacial friction law succeeds in obtaining better results.

Further investigation and parametric studies to precise the effect of the geometrical characteristics of the debris bed and flow conditions on the redistribution are foreseen in addition to sensitivity studies concerning interfacial friction laws and relative permeability and passability correlations.

Appendix

A.1 Quench Front Velocity Formula

$$v^{qf} = \frac{F^{vqf}}{E^{vqf}} = \frac{F_1 + F_2 + F_3}{E_1 + E_2 + E_3 + E_4} \quad (62)$$

where

$$\begin{aligned} F_1 &= [\varepsilon^0 \rho_l (S^b + S^c) v_l^{inj}] c_{pg} \Delta T_g \\ F_2 &= (1 - \alpha_1^c) \varepsilon^c S^c \rho_l v_{l1}^c \Delta h^{sat} \\ F_3 &= \varepsilon^b S^b \rho_l v_{l1}^b (h_g^{sat} - c_{pl} \Delta T_l^b) \end{aligned} \quad (63)$$

and

$$\begin{aligned} E_1 &= \rho_s c_{ps} [(1 - \varepsilon^c) S^c \Delta T_s^c + (1 - \varepsilon^b) S^b \Delta T_s^b] \\ E_2 &= \alpha_1^c \varepsilon^c S^c \rho_g c_{pg} \Delta T_g \\ E_3 &= (1 - \alpha_1^c) \varepsilon^c S^c \rho_l (\Delta h^{sat} + c_{pg} \Delta T_g) \\ E_4 &= \varepsilon^b S^b \rho_l (h_g^{sat} + c_{pg} \Delta T_g - c_{pl} \Delta T_l^b) \end{aligned} \quad (64)$$

A.2 Capillary Effects

The capillary pressure P_c is defined the pressure difference between the liquid and gas phases:

$$P_c = P_g - P_l \quad (65)$$

The capillary length for water is defined as:

$$l_c = \sqrt{\frac{\sigma}{(\rho_l - \rho_g)g}} \quad (66)$$

where σ is the surface tension. The capillary length for water is approximately 2 mm, and considering the bypass particles size (8 mm in diameter) are larger than l_c , the capillary effects can be neglected in this case. Hence, the pressure of the gas phase can be set equal to that of the liquid phase and thus the following equation holds in the bypass:

$$\frac{\partial P_g^b}{\partial z} \approx \frac{\partial P_l^b}{\partial z} \quad (67)$$

References

- Akers, A., McCardell, R., 1989. Core materials inventory and behavior. *Nuclear Technology* 87.
- Akers, D., Carlson, E., Cook, B., Ploger, S., Carlson, J., 1986. TMI-2 core debris grab samples examination and analysis. Technical Report GEND-INF-075. Sandia National Laboratory.
- Atkhen, K., Berthoud, G., 2003. Experimental and numerical investigations on debris bed coolability in a multidimensional and homogeneous configuration with volumetric heat source. *Nuclear Technology* 142.
- Brooks, R.H., Corey, A.T., 1966. Properties of porous media affecting fluid flow. *J. Irrig. Drain. Div. Am. Soc. civ. Engrs* IR2 92, 61–89.
- Broughton, J., Kuan, P., Petti, D., Tolman, E., 1989. A scenario of the Three Mile Island unit 2 accident. *Nuclear Technology* 87, 34–53.
- Carman, P., 1937. The determination of the specific surface area of powder I. *J. Soc. Chem. Ind.* 57, 225–234.
- Chikhi, N., Garcin, T., Foubert, F., March, P., Fichot, F., 2015. First experimental results of large scale debris bed reflood tests in the pearl facility, in: 16th International Topical Meeting on Nuclear Reactor Thermal Hydraulics (NURETH-16), Chicago, IL.
- Clavier, R., 2015. Étude expérimentale et modélisation des pertes de pression lors du renoyage d'un lit de débris. Ph.D. thesis. Institut National Polytechnique de Toulouse.
- Darcy, H., 1856. Fontaines Publiques de la Ville de Dijon. Libraire des Corps. Imperiaux des Ponts et Chaussées et des Mines, Paris.
- Ergun, S., 1952. Fluid flow through packed columns. *Chem. Eng. Prog.* 48, 89–94.
- Forchheimer, P., 1901. Wasserbewegung durch boden. *Z. Ver. Deutsch. Ing.* 45, 1782–1788.
- Fourar, M., Lenormand, R., 2000. Inertial effects in two-phase flow through fractures. *Oil and Gas Science and Technology* 55, 259–268.
- Hofmann, G., 1984. On the location and mechanisms of dryout in top-fed and bottom fed particulate beds. *Nuclear Technology* 65, 36–45.
- Hu, K., Theofanous, T., 1991. On the measurement of dryout in volumetrically heated coarse particle beds. *Int. J. Multiphase Flow* 65.
- Lasseux, D., Ahmadi, A., Arani, A., 2008. Two-phase inertial flow in homogeneous porous media: A theoretical derivation of a macroscopic model. *Transport in Porous Media* 75, 371–400.
- Lipinski, R., 1984. A coolability model for post-accident nuclear reactor debris. *Nuclear Technology* 65, 53–66.
- McCardell, R., Russell, M., Akers, D., Olsen, C., 1990. Summary of tmi-2 core sample examinations. *Nuclear Engineering and Design* 118, 441–449.

- Reed, A., 1982. The effect of channeling on the dryout of heated particulate beds immersed in a liquid pool. Ph.D. thesis. MIT. Cambridge (USA).
- Reed, A., Boldt, K., Gorham-Bergeron, E., Lipinski, R., Schmidt, T., 1985. DCC-1/DCC-2 degraded core coolability analysis. Technical Note NUREG/CR-4390-R3. Sandia National Labs.
- Repetto, G., Chikhi, N., Fichot, F., 2013. Main outcomes on debris bed cooling from prelude experiments. in 6th european review meeting on severe accident researchexperimental program on debris reflooding (pearl) - results on prelude facility, in: 6th European Review meeting on Severe Accident Research (ERMSAR-2013).
- Repetto, G., Garcin, T., Eymery, S., March, P., Fichot, F., 2011. Experimental program on debris reflooding (pearl) - results on prelude facility, in: 14th International Topical Meeting on Nuclear Reactor Thermal Hydraulics (NURETH-14), Toronto, Canada.
- Schäfer, P., Groll, M., Kulenovic, R., 2006. Basic investigations on debris coolability. Nuclear Engineering and Design 236, 2104–2116.
- Schmidt, W., 2007. Interfacial drag of two-phase flow in porous media. Int. J. Multiphase Flow 33, 638–657.
- Schulenberg, T., Müller, U., 1984. A Refined Model for the Coolability of Core Debris with Flow Entry from the Bottom. 6th Information Exchange Meeting on Debris Coolability, Los Angeles .
- Schulenberg, T., Müller, U., 1987. An improved model for two-phase flow through beds of coarse particles. Int. J. Multiphase Flow 13, 87–97.
- Stenne, N., Pradier, M., Olivieri, J., Eymery, S., Fichot, F., March, P., Fleurot, J., 2009. Multi-dimensional reflooding experiments: the pearl program, in: OECD/NEAEC/SARNET2 Workshop, In Vessel Coolability, Paris (France).
- Tung, V., Dhir, V., 1983. Quenching of a hot particulate bed by bottom quenching, in: ASME-JSME Thermal Engineering Joint Conference, Honolulu, Hawa.
- Tung, V., Dhir, V., 1988. A hydrodynamic model for two-phase flow through porous media. Int. J. Multiphase Flow 14, 47–65.
- Tutu, N., Ginsberg, T., Klein, J., Klages, J., Schwarz, C., 1984. Debris bed quenching under bottom flood conditions. Technical Report NUREG/CR-3850. Brookhaven National Labs.
- Whitaker, S., 1996. The forchheimer equation : a theoretical development. Transport in Porous Media 25, 27–61.